Journal of Dermatological Science 97 (2020) 50–56

Contents lists available at ScienceDirect

Journal of Dermatological Science

journal homepage: www.jdsjournal.com

Original Article

Reduced stratum corneum acylceramides in autosomal recessive congenital ichthyosis with a *NIPAL4* mutation

Yuya Murase[a], Takuya Takeichi[a,*], Akane Kawamoto[b], Kana Tanahashi[a], Yusuke Okuno[c], Hiroyuki Takama[d], Eri Shimizu[e], Junko Ishikawa[b], Tomoo Ogi[f], Masashi Akiyama[a,*]

[a] Department of Dermatology, Nagoya University Graduate School of Medicine, Nagoya, Japan
[b] Biological Science Research Laboratories, Kao Corporation, Haga, Japan
[c] Center for Advanced Medicine and Clinical Research, Nagoya University Hospital, Nagoya, Japan
[d] Department of Dermatology, Aichi Medical University, Nagakute, Japan
[e] Analytical Science Research Laboratories, Kao Corporation, Haga, Tochigi, Japan
[f] Department of Genetics, Research Institute of Environmental Medicine, Nagoya University, Nagoya, Japan

ARTICLE INFO

Article history:
Received 10 September 2019
Received in revised form 25 November 2019
Accepted 1 December 2019

Keywords:
Autosomal recessive congenital ichthyosis
Ceramide
NIPAL4
Skin barrier
Stratum corneum
Acylceramide

ABSTRACT

Background: NIPAL4, encoding the NIPA-like domain containing 4 protein (NIPAL4), is one of the causative genes of autosomal recessive congenital ichthyosis (ARCI). The physiological role of NIPAL4 and the pathogenetic mechanisms of ARCI caused by *NIPAL4* mutations remain unclear.
Objective: To clarify the changes of ceramide components in the lesional stratum corneum (SC) and the gene expression profile in the lesional skin of an ARCI patient with a novel frameshift mutation in *NIPAL4*.
Methods: We performed ultrastructural and immunohistochemical analyses of the skin. We used RNA sequencing to determine the mRNA expression in the skin of the patient and healthy individuals. We investigated ceramide components using tape stripped SC samples from the patient.
Results: mRNA expression profiling in the patient's skin showed significant upregulation of IL-17/TNFα-related genes (*IL17C*, *IL36A*, *IL36G*, *S100A7A*, *S100A9*) and psoriasis hallmark genes (*VNN3, LCE3D, PLA2G4D*), and significant downregulation of lipid-associated genes (*GAL*, *HAO2*, *FABP7*). Ceramide analysis in the patient's SC revealed amounts of CER[NS] with carbon chain-length (C) 32–52 were increased, while amounts of most acylceramide with C66:2 - C72:2 were reduced relatively to those in healthy individuals. After the retinoid treatment, CER[NS] with carbon chains C46–54, CER[EOH] and CER [EOP] increased.
Conclusion: IL-17C and IL-36 family cytokines might be involved in the pathogenetic process of ARCI with *NIPAL4* mutations. Reduced amounts of the acylceramides in the SC are associated with the skin phenotype due to *NIPAL4* mutations. Efficacy of the oral retinoid treatment might be due to restored amounts of CER[EOH] and CER[EOP] in the SC.

1. Introduction

NIPAL4, the gene encoding the NIPA-like domain containing 4 protein (NIPAL4), is one of the causative genes of autosomal recessive congenital ichthyosis (ARCI) [1]. The physiological role of NIPAL4 and the pathogenetic mechanisms of ARCI caused by *NIPAL4* mutations remain unclear, although some recent studies have indicated that NIPAL4 may be a putative Mg^{2+} transporter [2,3] and that loss-of-function of NIPAL4 might lead to a failure of differentiation-dependent gene expression in keratinocytes, resulting in a defective acylceramide synthesis by keratinocytes [3]. NIPAL4 is present in other organs and tissues, although its mRNA is expressed most strongly in the skin (Ref. THE HUMAN PROTEIN ATLAS (https://www.proteinatlas.org/)). However, no other organ involvement has been reported in autosomal recessive congenital ichthyosis patients with *NIPAL4* mutations [4–6].

The skin permeability barrier is essential for prevention of water loss and penetration of harmful substances. Corneocytes are surrounded by corneocyte lipid envelope (CLE; protein-bound ceramides), and extracellular, multilayered lipid structures known as extracellular lipid lamellae [7]. The extracellular lipid lamellae, which is mainly composed of ceramide, cholesterol, and free fatty

Abbreviations: ARCI, autosomal recessive congenital ichthyosis; NIPAL4, NIPA-like domain containing 4 protein, acylceramide.

* Corresponding authors at: Takuya Takeichi, Department of Dermatology, Nagoya University, Graduate School of Medicine, 65 Tsurumai-cho, Showa-ku, Nagoya 466-8550, Japan.
E-mail addresses: takeichi@med.nagoya-u.ac.jp (T. Takeichi), makiyama@med.nagoya-u.ac.jp (M. Akiyama).

https://doi.org/10.1016/j.jdermsci.2019.12.001
0923-1811/

acids, plays an important role in the formation of barrier function in the epidermis [8]. Most of the genes causative of ARCI are associated with epidermal ceramide synthesis and metabolism, and CLE formation. In ARCI cases with mutations in such epidermal lipid-associated causative genes, skin barrier defects due to deficiency of the epidermal ceramides, especially acylceramides, and malformation of CLE are thought to cause ARCI phenotypes [7,9–13].

In the present study, we have analyzed detailed ceramide components in the stratum corneum (SC) of an ARCI patient with a homozygous *NIPAL4* mutation before and after oral retinoid treatment. In addition, we have investigated the gene expression profile in the lesional skin of the patient.

2. Materials and methods

2.1. Report of a case

A 51-year-old male, the first child of related parents, had had an ARCI phenotype since birth. The ichthyotic phenotype, with moderate hyperkeratosis in erythrodermic skin over almost the entire body, was present from the neonatal period, although he was not born as a collodion baby. On examination, he had generalized dry skin with white to gray scales and linear palmoplantar hyperkeratosis (Figs. 1 and 2). The present patient showed no symptoms other than skin lesions. Histopathologically, the affected skin showed acanthosis with compact hyperkeratosis in the epidermis, suggesting a reduced amount of the intercellular lipids in the SC (Fig. 3A and B). Characteristic histopathological features of psoriasis, including parakeratosis, inflammatory cell infiltration in the superficial dermis or Munro's microabscesses, were not observed in the skin biopsy samples from the upper arm or the sole. In addition, characteristic histopathological features of pityriasis rubra pilaris, including alternating parakeratosis and hyperkeratosis or follicular keratin plugs, were not observed in the skin biopsy samples. (Fig. 3A and B). Ultrastructural observations showed defective intercellular lipid layer (Suppl. Fig. 1). He was treated with a low-dose etretinate (15 mg/day), leading to sufficient control (Fig. 2).

2.2. Electron microscopy (EM)

Skin samples were fixed in 2.5 % (w/v) glutaraldehyde solution, post-fixed in 0.5 % (w/v) ruthenium tetroxide (RuO_4), dehydrated and embedded in Epon812 (TAAB Laboratories, Berks, UK). All samples were ultra-thin sectioned at a thickness of 75 nm and stained with uranyl acetate and lead citrate. Photographs were taken using a JEM1400 transmission electron microscope (JEOL Ltd., Tokyo, Japan).

2.3. Mutation detection

Ethical approval was obtained and all research was performed in accordance with the principles of the Declaration

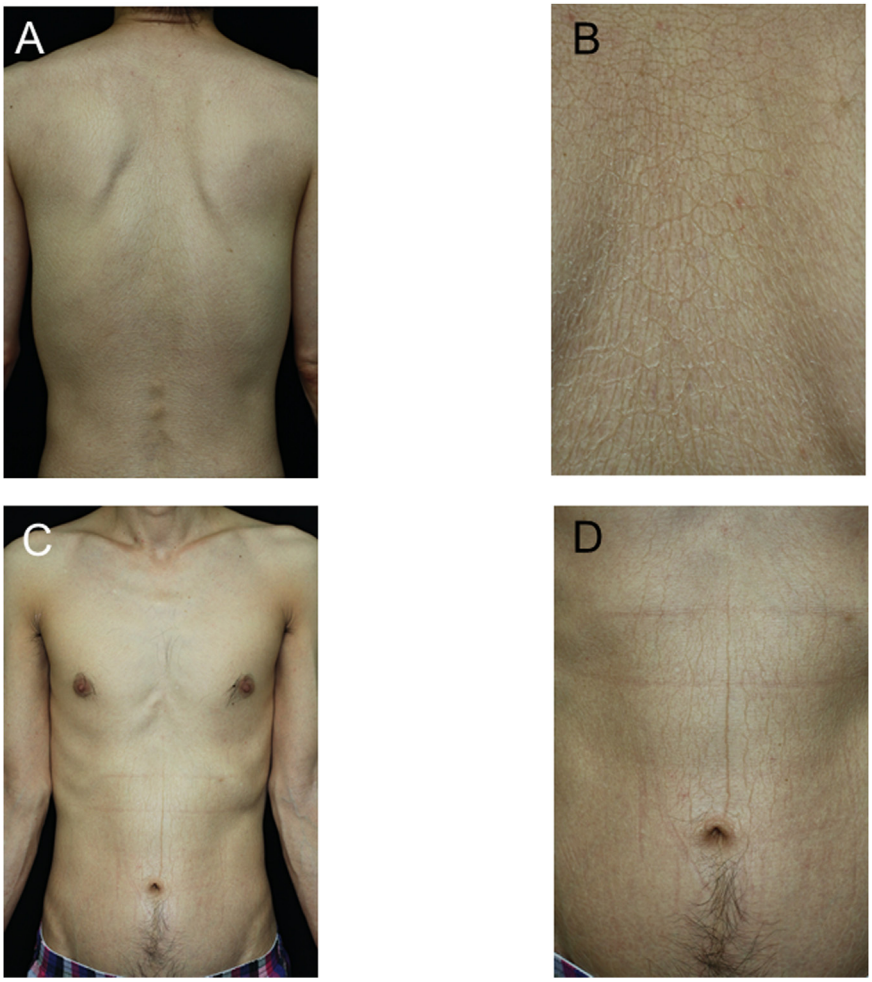

Fig. 1. The ichthyotic skin lesions of the patient.
He had generalized, moderate hyperkeratosis with white to gray scales (A, B, back; C, chest and abdomen; D, abdomen).

Fig. 2. Clinical features of the patient before, one month and two months after the oral retinoid treatment.
A–C, Hyperkeratotic and scaly lesions in the forearm, the upper arm, the palm and the sole of the patient before (A), one month (B) and two months (C) after the oral etretinate treatment. The patient's skin symptoms were gradually improved for 2 months with the oral etretinate treatment.

of Helsinki. To identify the pathogenetic mutation of the patient, whole-exome sequencing was performed using DNA extracted from peripheral blood from the patient and his mother as described previously with slight modifications [14]. Briefly, genomic DNA were enriched using the Agilent SureSelect Human All Exon Kit v5 (Agilent, Santa Clara, CA). The enriched genomic fragments were sequenced on the Illumina HiSeq 2500 sequencer (Illumina, San Diego, CA, USA) to generate ~150x coverage of 150-bp paired-end reads. Exome data were analysed with a Broad Institute's standard exome pipeline. After variant annotation, candidate gene mutations were prioritized by screening for variants reported as causative genes of ichthyosis. The identified mutations were verified by subsequent Sanger sequencing.

2.4. RNA sequencing

We isolated total RNA from the skin samples using the RNeasy Mini Kit (Qiagen, Hiden Germany). The integrity of the extracted RNA was measured by an Agilent 2200 TapeStation system and RNA ScreenTape (Agilent, Santa Clara, CA). Nondirectional sequencing libraries were prepared using the NEBNext Ultra II RNA Prep Kit for Illumina and the NEBNext Poly(A) mRNA Magnetic Isolation Module (New England Biolabs, Ipswich, MA) according to the manufacturer's instructions. Next-generation sequencing was performed using a HiSeq2500 sequencer to obtain 2×100-bp paired end reads. An average of 50 million paired reads per sample were aligned to the hg19 reference genome using tophat2 (https://ccb.jhu.edu/software/tophat/) with default parameters. The

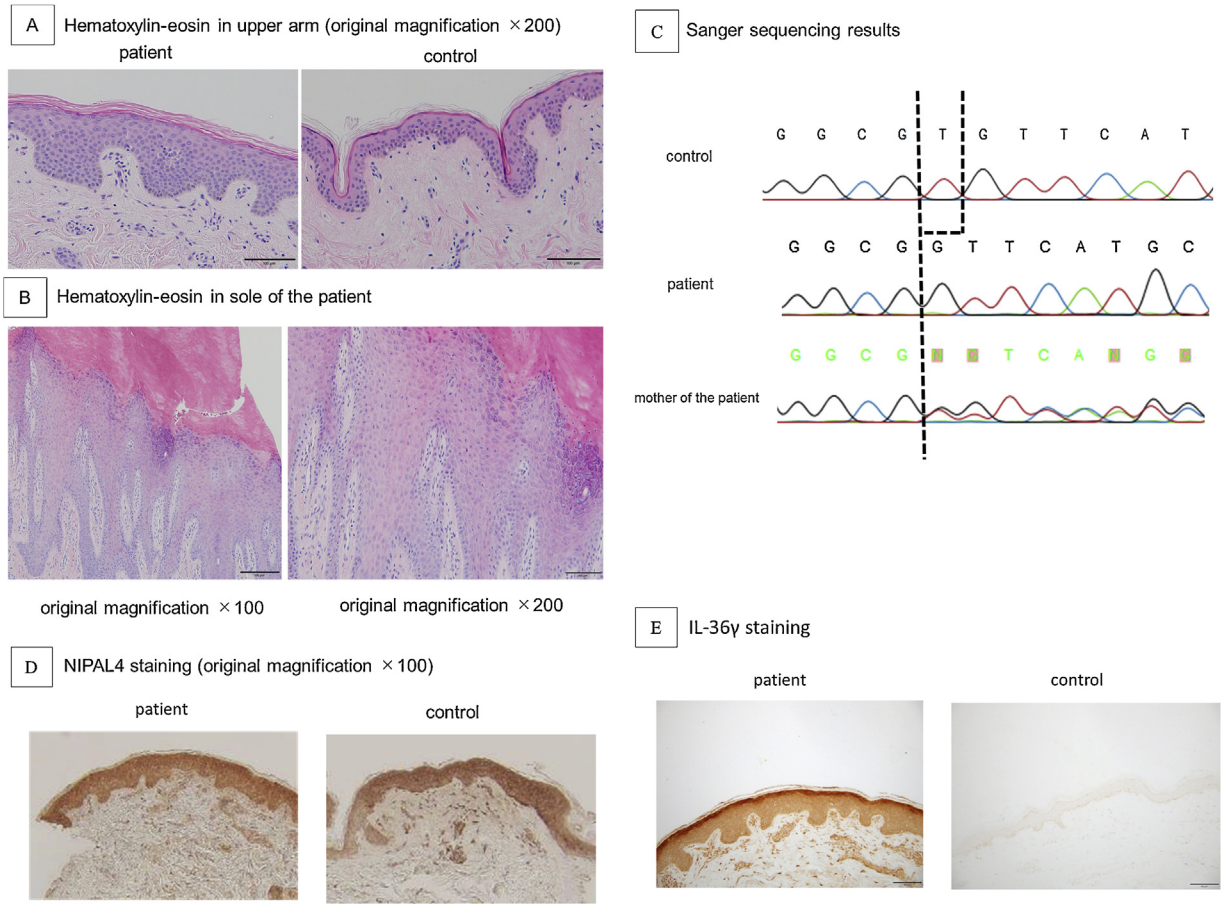

Fig. 3. Histopathological and immunohistochemical findings and the *NIPAL4* mutation causative of ARCI in the present patient.
A, B, Light microscopy shows compact hyperkeratosis in the patient's epidermis in the upper arm and the sole. (hematoxylin-eosin (HE)) None of the characteristic histopathological features of psoriasis or pityriasis rubra pilaris, including inflammatory cell infiltration in the superficial dermis, Munro's microabscesses, parakeratosis, and hypogranulosis and follicular keratin plugs, are observed in the upper arm or the sole.
C, Sanger sequencing of the patient's genomic DNA revealed a homozygous mutation c.1202delT in *NIPAL4* in the patient. His mother was heterozygous for the identical mutation.
D, The epidermis of the patient's skin was positively stained with the anti-NIPAL4 antibody (original magnification ×100). There was no significant difference in NIPAL4 staining patterns and strength between the patient's skin and a healthy control skin.
E, The patient's epidermis was strongly positive for anti-IL-36γ staining, compared with the faint staining in the epidermis of a healthy control skin sample (original magnification, × 100).

number of reads for each gene was counted by HTSeq (https://htseq.readthedocs.io/) and differential expression was calculated based on the negative binomial test using DESeq2 (https://bioconductor.org/packages/release/bioc/html/DESeq2.html). We considered a p-value of <0.1 after multiple testing correction to be significant.

2.5. Immunohistochemical analyses

Skin punch biopsy specimens were obtained from the patient and normal controls under local anesthesia. Immunofluorescence staining using a rabbit polyclonal anti-NIPAL4 antibody (orb27926, Biorbyt, LLC, San Francisco, CA, USA; dilution 1:100), and a mouse monoclonal anti-IL-36 gamma antibody (ab156783, Abcam, Cambridge, MA, USA; dilution 1:150) was performed, as described elsewhere [15].

2.6. Tape stripping and lipid analysis by liquid chromatography-mass spectrometry

To examine the ceramide classes in the SC, tape stripping was performed by pressing and stripping an adhesive acrylic film (456#40; Teraoka Seisakusho, Tokyo, Japan) on the skin of the forearm and upper arm of the patient, the patient's mother and 13 healthy individuals as controls. Five consecutive tape strips (25 × 15 mm) were obtained from each individual. The samples were then subjected to liquid chromatography-mass spectrometry analysis to assess the levels of 11 major ceramide species [16,17]. Each strip was cut into two half-strips: one for lipid analysis and the other for protein analysis.

The tape strips were dissolved in 2 ml of chloroform/methanol/2-propanol (10:45:45, volume/volume/volume). *N*-heptadecanoyl-D-erythro-sphingosine (d18:1/17:0) (Avanti Polar Lipids) was added as an internal control, and its final concentration was 50 nmol/L. This lipid solution was subjected to reverse-phase liquid chromatography/ mass spectrometry. The system was an Agilent 6130 Series LC/MSD SL system equipped with a multi-ion source, ChemStation software, an Agilent 1260 Infinity Series LC (Agilent Technologies) and an L-column octadecylsilyl (2.1-mm internal diameter × 150 mm; Chemicals Evaluation and Research Institute). Chromatographic separation of the lipids was achieved at a flow rate of 0.2 ml/minute using the mobile phase of a binary gradient solvent system. Each ceramide species was detected by selected ion monitoring of *m/z* $[M + CH_3COO]^-$. Soluble proteins were extracted from the other half-strip with a 0.1-mol/L NaOH 1 % sodium dodecyl sulfate aqueous solution at 60 °C for 150 min. The

extract solutions were then neutralized with an HCl aqueous solution. After that, soluble proteins were measured using a BCA protein assay kit (Thermo Fisher Scientific, Waltham, MA).

3. Results

3.1. Detection of a novel frameshift mutation in NIPAL4

Whole-exome and Sanger sequencing of the patient's genomic DNA revealed a novel homozygous mutation c.1202delT (p.Val401Glyfs*47) in *NIPAL4* (Fig. 3C). The c.1202delT mutation is not found in the Human Genetic Variation Database, which includes 1,208 exome datasets from Japanese controls (http://www.hgvd.genome.med.kyoto-u.ac.jp/index.html), nor in the gnomAD Database (http://gnomad.broadinstitute.org/), which includes data for 123,136 whole exomes and 15,496 whole genomes. In addition, one duplication mutation, c.1193dupT (p.Val401Argfs*36), which causes a frameshift from the Val401 residue identical to the frameshift starting site by the present mutation, was reported as a causative mutation in *NIPAL4* in an autosomal recessive congenital ichthyosis patient [18]. The present *NIPAL4* mutation is a small deletion mutation resulting in frameshift and premature termination. Thus, we consider that the mutant protein must be shorter than the wild-type protein. The truncated NIPAL4 protein is expected to lack a part of the ninth transmembrane domain and the entire C-terminal intracytoplasmic region [19]. The Val401 residue is located in the C-terminal transmembrane domain of NIPAL4, and we assume that the frameshift from the residue and the truncation of the C-terminal region might be deleterious to NIPAL4 function. From these findings, we consider that the present truncating *NIPAL4* mutation is truly pathogenic. Whole-exome sequencing of the patient's genomic DNA revealed no pathogenic mutation in either the desmoplakin gene (*DSP*) or the desmoglein-1 gene (*DSG1*). Immunohistochemical analyses showed that there was no significant difference in the NIPAL4 staining pattern and strength between the patient's and healthy control skin samples (Fig. 3D). In addition, we performed quantitative RT-PCR in order to evaluate the mutant *NIPAL4* mRNA expression in the patient's skin. The mutant *NIPAL4* mRNA expression in the present patient's skin was found to be at a level similar to those of wild-type alleles in the normal control samples (Suppl. Fig. 2). Thus, we speculate that nonsense-mediated mRNA decay (NMD) may not occur in the present case and that a decent amount of NIPAL4 truncated protein might be present in the patient's skin, although we cannot exclude completely the possibility of NMD in the present patient because NMD can be excluded only when no increase of mutant mRNA is observed after inhibition of NMD and we have not performed NMD inhibition experiments in the present case. The immunohistochemical analysis showed no decrease in NIPAL4 expression levels in the patient's lesional skin, because the antibodies against NIPAL4 used in the present study were not specific to the C-terminal of NIPAL4. On the other hand, the patient's skin was strongly positive for IL36γ, compared with healthy control skin samples (Fig. 3E).

3.2. mRNA expression profiling in the patient's skin

RNA sequencing analyses of mRNA extracted from the skin punch biopsy specimens showed significant upregulation of IL-17/TNFα-related genes (*IL17C*, *IL36A*, *IL36G*, *S100A7A*, *S100A9*) and psoriasis hallmark genes (*VNN3, LCE3D, PLA2G4D*) (Table 1, Suppl. Table 1), and significant downregulation of lipid-associated genes (*GAL*, *HAO2*, *FABP7*) (Table 1, Suppl. Table 2) in the patient's skin compared with those in normal control skin samples. There were no significant differences in mRNA expression of differentiation marker genes (*LOR*, *FLG*, and *PPL*) and ARCI-causative genes between the patient's skin and the control skin samples (Suppl. Table 3).

Table 1
Significantly upregulated IL-17/TNFα-related genes, psoriasis hallmark genes and downregulated lipid-associated genes in the patient with a *NIPAL4* mutation compared to the those of healthy individuals.

Gene	log2Fold change	padj
upregulated		
IL36A	10.11947657	5.02E-18
S100A7A	4.138600176	2.50E-17
VNN3	4.873737416	4.24E-10
IL36G	2.995048792	1.37E-09
S100A9	2.819372931	3.13E-07
LCE3D	2.284500298	1.33E-05
IL17C	4.083101697	0.000137582
PLA2G4D	2.186189356	0.00025858
downregulated		
GAL	Inf	2.66E-10
HAO2	6.279592002	0.001220711
FABP7	2.759705829	0.004124171

Abbreviations: Inf, infinite.

3.3. Analysis of ceramides in the SC of the patient's skin

Although a total amount of ceramide in the SC from the patient's forearm was almost the same as those from healthy individuals, the total amount of ceramides in the SC from the upper arm of the patient was reduced compared with those of healthy individuals (Fig. 4A). Each ceramide class is named using combination abbreviations for the constituent fatty acids (N, non-hydroxy fatty acid; A, α-hydroxy fatty acid; EO, esterified ω-hydroxy fatty acid) and long chain bases (S, sphingosine; DS, dihydrosphingosine; P, phytosphingosine; H, 6-hydroxysphingosine) [20]. In both the forearm and the upper arm of the patient, the amount of CER[NS] was significantly increased, while those of CER[AH], CER[AP], CER[EOH] and CER[EOP] were reduced (Fig. 4B). Moreover, in the upper arm, the amounts of CER[NH], CER[NP] and CER[EOS] were also reduced compared with those in healthy individuals (Fig. 4B). Furthermore, in both sites, amounts of most CER[NS]s with carbon chain-length (C) 32–52 were increased (Fig. 4C), while amounts of most acylceramides (CER[EOS], CER[EOH] and CER[EOP]) with C66:2 (66 carbon atoms and two unsaturated bonds) - C72:2 were reduced (Fig. 5).

After the oral etretinate treatment, in the both lesions, the amounts of CER[EOH] and CER[EOP] were increased and got close to those of the healthy individuals (Fig. 4B). Moreover, in the upper arm, the amounts of CER[NH] and CER[NP] were also increased after the treatment, while that of CER[NS] was reduced in the forearm after the treatment (Fig. 4B). The composition of the CER[NS] with carbon chains C32-45 was reduced, while those of the CER[NS] with carbon chains C46–54 increased (Suppl. Fig. 3). Amounts of CER[EOH] and CER[EOP] with C66:2-70:2 were increased in the lesional skin of both the forearm and the upper arm after the treatment (Fig. 5). These results suggested that the fatty acid elongation activity might improve by the treatment.

4. Discussion

Although Fischer reported that mutations in *NIPAL4* have been identified in approximately 16 % of patients with ARCI [21], the carrier rate of ichthyosis-causing *NIPAL4* mutations is thought to be extremely low in Japan or Asia [19]. Most ARCI-causative genes have been reported to be involved in the formation of acylceramide or protein-bound ceramide [3,10]. According to the results of lipid analysis in the present study, the amount of acylceramides (CER[EOH], CER[EOP] and CER[EOS]) which are synthesized in the

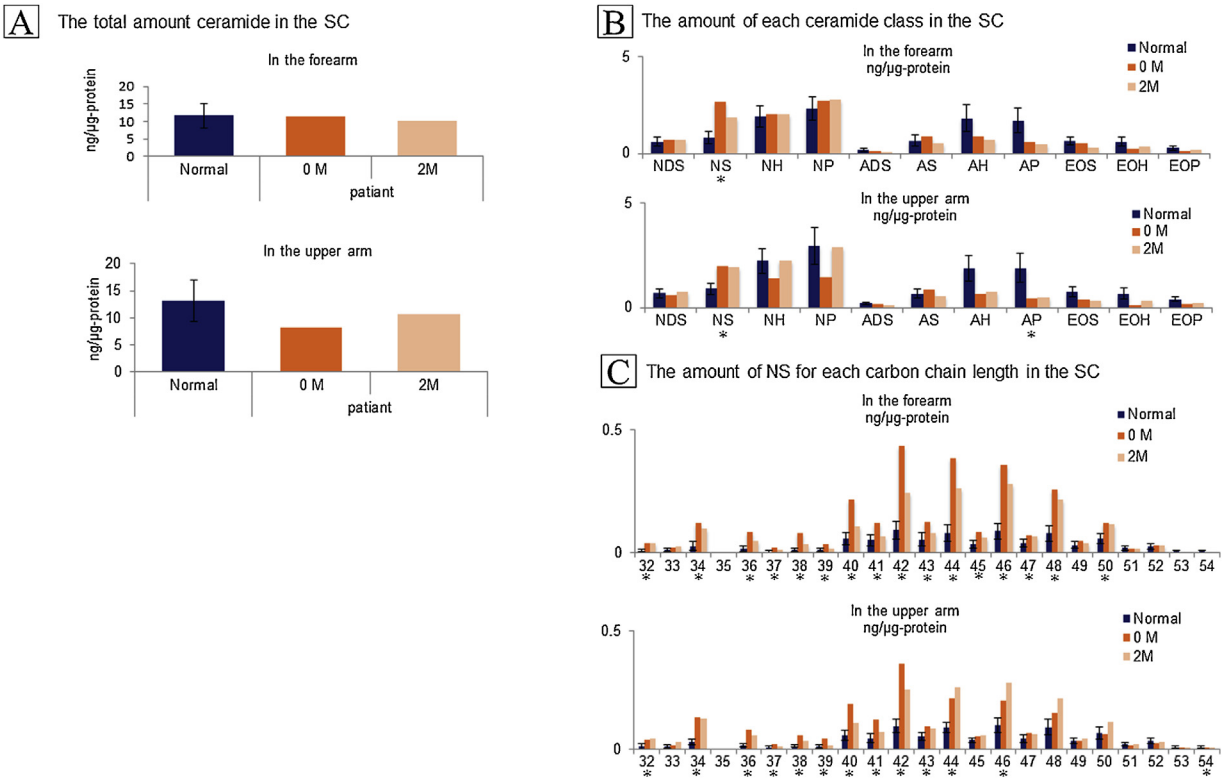

Fig. 4. Analysis of the SC lipid using tape stripped stratum corneum samples from the patient and 13 healthy individuals.
A) In the upper arm of the patient, the total amount of ceramide was reduced compared with those in the healthy controls. After treatment for two months (2 M), in the upper arm of the patient, the reduction of total amount of ceramides was not seen, whereas there was no significant change in the forearm. B) The amount of CER[NS] was increased both in the forearm and in the upper arm of the patient, whereas those of CER[AH], CER[AP], CER[EOH] and CER[EOP] were reduced in both lesions. After the treatment, in both lesions, the amounts of CER[EOH] and CER[EOP] were increased. An asterisk (*) under the ceramide classes indicates that there were ± 2 SD difference between normal control and the patient before the treatment (0 M). C) The compositions of the CER[NS] with C32-35 were reduced, while those of the CER[NS] with C 46–54 were not. Asterisks (*) under the carbon chain lengths indicate that there were more than ±2SD difference between normal controls and the patient before the treatment (0 M).

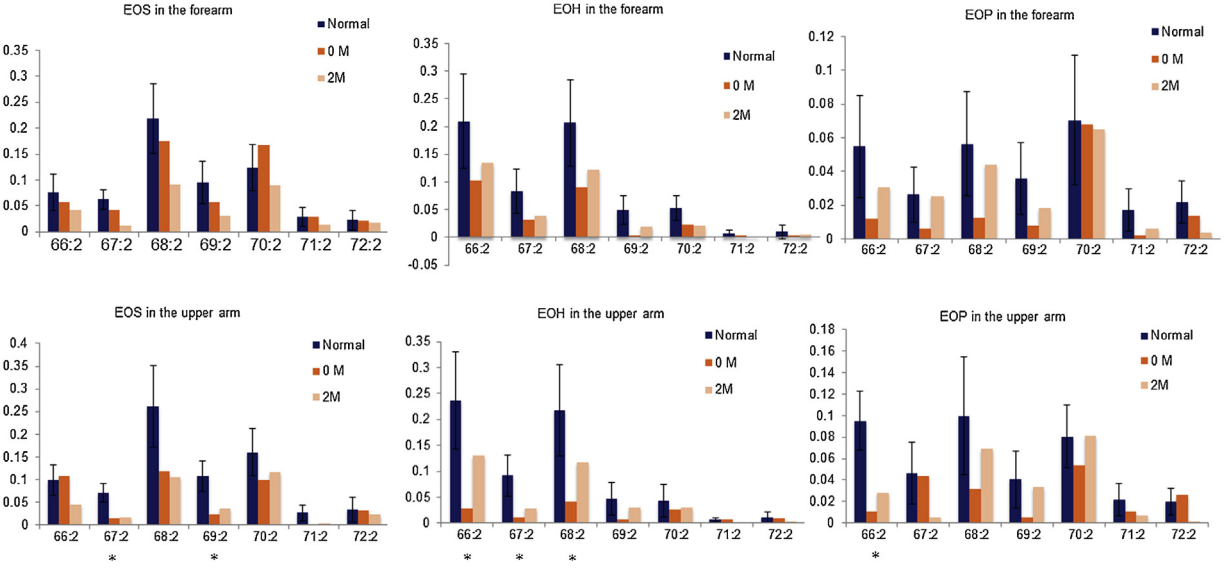

Fig. 5. Analysis of acylceramides in the SC using tape stripped samples.
Before the treatment (0 M), CER[EOS], CER[EOH], and CER[EOP] with some carbon chain-lengths were significantly reduced in the upper arm of the patient. Asterisks (*) under the ceramide classes indicate that there were more than ±2SD difference between normal control and the patient's specimens before the treatment (0 M). After the oral etretinate treatment for two months (2 M), CER[EOS] with C66:2-70:2 was reduced in the forearm, and was slightly reduced or almost stable in the upper arm, compared with that before the treatment (0 M). On the other hand, most CER[EOH] and CER[EOP] with C66:2-70:2 was increased after the treatment (2 M).

upper layer of stratum spinosum and stratum granulosum (SG) was reduced in the SC of the present patient. After the oral etretinate treatment, among CER[NS], the composition of CER[NS] with short carbon chain-length fatty acids was reduced, and that of CER[NS] with long carbon chain-length fatty acids was increased. These changes might be resulted from improvement of fatty acids elongation activity by the fatty acid elongases (e.g. ELOVL1, ELOVL4).

IL-36 was reported to promote a strong pro-inflammatory signature in primary keratinocytes and perturb skin differentiation. The skin samples from the present case showed the significantly increased mRNA expressions of *IL36A* and *IL36 G*. These findings are consistent with the results of quantitative RT-PCR analyses in previous reports [22,23]. Furthermore, the protein expression of IL36γ was higher in the skin of the present patient than that in the normal control specimens. Thus, upregulated IL36γ might be involved in the pathogenesis of ARCI in the present case. Malik et al. reported that increased mRNA and protein expression of IL-36 family members and IL-36 receptor was significantly correlated with ichthyosis severity and transepidermal water loss in various ichthyosis subtypes [23]. Significant upregulation of IL-17/TNF-α-related genes and psoriasis hallmark genes has been reported in autosomal recessive congenital ichthyosis patients with mutations in causative genes including *NIPAL4* [23–25]. Thus, we think the present upregulation of IL-17/TNF-α-related genes and psoriasis hallmark genes is not specific to ichthyosis patients with *NIPAL4* mutations.

After the successful etretinate treatment, the amount of CER[EOH] and CER[EOP] were increased in the patient's SC, although CER[EOS] was not increased in the present study. We speculate that etretinate induced normal differentiation of the patient's epidermal keratinocytes, resulting in the increase of ceramide amounts in the patient's SC. Increased amounts of not only CER[EOS], but also CER[EOH] and CER[EOP] were reported to be strongly correlated with SC barrier functions in Japanese males [16]. Thus, our findings suggest that the increased amounts of CER[EOH] and CER[EOP] after the treatment may be associated with improvement of skin symptoms in the patient with the *NIPAL4* mutation.

mRNA expression profiling in the present patient skin suggested that IL-17C and IL36 family cytokines might be involved in the pathogenetic process of ARCI with *NIPAL4* mutations. Furthermore, the present ceramide analysis revealed that reduced amounts of the acylceramides, CER[EOS], CER[EOH] and CER[EOP], in the SC are associated with the skin phenotype of ARCI due to *NIPAL4* mutations. In addition, improvement of skin symptoms in ARCI with *NIPAL4* mutations by the oral retinoid treatment might be due to restored amounts of CER[EOH] and CER[EOP] in the SC.

Declaration of Competing Interest

The authors declare that there are no conflicts of interest.

Acknowledgments

This work was supported by funding from the Japan Agency for Medical Research and Development (AMED)JP18ek0109295h0002 and 18ek0109281h0002 to M.A. This work was also supported by Grant-in-Aid for Scientific Research (B)18H02832 to M.A., and by Grant-in-Aid for Young Scientists18K16058 to T.T. from the Japan Society for the Promotion of Science (JSPS). This investigation was supported in parts by The Mochida Memorial Foundation for Medical and Pharmaceutical Research, The Uehara Memorial Foundation and The Kanae Foundation for the Promotion of Medical Science.

Appendix A. Supplementary data

Supplementary material related to this article can be found, in the online version, at doi:https://doi.org/10.1016/j.jdermsci.2019.12.001.

References

[1] T. Takeichi, M. Akiyama, Inherited ichthyosis: non-syndromic forms, J. Dermatol. (3) (2016) 242–251.
[2] G.A. Quamme, Molecular identification of ancient and modern mammalian magnesium transporters, Am. J. Physiol., Cell Physiol. 298 (2010) C407–C429.
[3] Y. Honda, T. Kitamura, T. Naganuma, T. Abe, Y. Ohno, T. Sassa, A. Kihara, Decreased skin barrier lipid acylceramide and differentiation-dependent gene expression in icthyosis gene Nipal4-Knockout mice, J. Invest. Dermatol. 138 (4) (2018) 741–749.
[4] V. Oji, G. Tadini, M. Akiyama, C. Blanchet Bardon, C. Bodemer, E. Bourrat, et al., Revised nomenclature and classification of inherited ichthyoses: results of the first ichthyosis consensus conference in Soreze 2009, J. Am. Acad. Dermatol. 63 (2010) 607–641.
[5] H. Traupe, J. Fischer, V. Oji, Nonsyndromic types of ichthyoses - an update, J. Dermatol. Ges. 12 (2) (2014) 109–121.
[6] L. Youssefian, H. Vahidnezhad, A.H. Saeidian, A. Touati, S. Sotoudeh, H. Mahmoudi, et al., Autosomal recessive congenital ichthyosis: genomic landscape and phenotypic spectrum in a cohort of 125 consanguineous families, Hum. Mutat. 40 (3) (2019) 288–298.
[7] A. Muñoz-Garcia, C.P. Thomas, D.S. Keeney, Y. Zheng, A.R. Brash, The importance of the lipoxygenase-hepoxilin pathway in the mammalian epidermal barrier, Biochim. Biophys. Acta 1841 (3) (2014) 401–408.
[8] K.R. Feingold, P.M. Elias, Role of lipids in the formation and maintenance of the cutaneous permeability barrier, Biochim. Biophys. Acta 1841 (3) (2014) 280–294.
[9] S. Grond, T.O. Eichmann, S. Dubrac, D. Kolb, M. Schmuth, J. Fischer, et al., PNPLA1 deficiency in mice and humans leads to a defect in the synthesis of Omega-O-Acylceramides, J. Invest. Dermatol. 137 (2) (2017) 394–402.
[10] A. Kihara, Synthesis and degradation pathways, functions, and pathology of ceramides and epidermal acylceramides, Prog. Lipid Res. 63 (2016) 50–69.
[11] M. Akiyama, Corneocyte lipid envelope (CLE), the key structure for skin barrier function and ichthyosis pathogenesis, J. Dermatol. Sci. 88 (1) (2017) 3–9.
[12] T. Hirabayashi, T. Anjo, A. Kaneko, Y. Senoo, A. Shibata, H. Takama, et al., PNPLA1 has a crucial role in skin barrier function by directing acylceramide biosynthesis, Nat. Commun. 8 (2017)14609.
[13] B. Breiden, K. Sandhoff, The role of sphingolipid metabolism in cutaneous permeability barrier formation, Biochim. Biophys. Acta 1841 (3)(2014) 441–452.
[14] T. Takeichi, Y. Okuno, A. Kawamoto, T. Inoue, E. Nagamoto, C. Murase, et al., Reduction of stratum corneum ceramides in Neu-Laxova syndrome caused by phosphoglycerate dehydrogenase deficiency, J. Lipid Res. 59 (12) (2019) 2413–2420.
[15] T. Takeichi, C. Katayama, T. Tanaka, Y. Okuno, N. Murakami, M. Kono, et al., A novel IFIH1 mutation in the pincer domain underlies the clinical features of both Aicardi-Goutières and Singleton-Merten syndromes in a single patient, Br. J. Dermatol. 178 (2) (2019) e111–e113.
[16] J. Ishikawa, Y. Shimotoyodome, S. Ito, Y. Miyauchi, T. Fujimura, T. Kitahara, et al., Variations in the ceramide profile in different seasons and regions of the body contribute to stratum corneum functions, Arch. Dermatol. Res. 305 (2) (2013) 151–162.
[17] Y. Ohno, S. Nakamichi, A. Ohkuni, N. Kamiyama, A. Naoe, H. Tsujimura, et al., Essential role of the cytochrome P450 CYP4F22 in the production of acylceramide, the key lipid for skin permeability barrier formation, Proc. Natl. Acad. Sci. U. S. A. 112 (2019) 7707–7712.
[18] H. Bučková, H. Nosková, R. Borská, K. Réblová, B. Pinková, E. Zapletalová, et al., Autosomal recessive congenital ichthyoses in the Czech Republic, Br. J. Dermatol. 174 (2) (2016) 405–407.
[19] M. Kusakabe, M. Nagai, E. Nakano, O. Jitsukawa, C. Nishigori, K. Yamanishi, A japanese case of ichthyosiform erythroderma with a novel mutation in NIPAL4/Ichthyin, Acta Derm. Venereol. 97 (3) (2017) 397–398.
[20] T. Hirabayashi, M. Murakami, A. Kihara, The role of PNPLA1 in ω-O-acylceramide synthesis and skin barrier function, Biochim. Biophys. Acta. Mol. Cell Biol. Lipids. 1864 (6) (2019) 869–879.
[21] J. Fischer, Autosomal recessive congenital ichthyosis, J. Invest. Dermatol. 129 (6) (2009) 1319–1321.
[22] C.M. Henry, G.P. Sullivan, D.M. Clancy, I.S. Afonina, D. Kulms, S.J. Martin, Neutrophil-derived proteases escalate inflammation through activation of IL-36 family cytokines, Cell Rep. 14 (4) (2016) 708–722.
[23] K. Malik, H. He, T.N. Huynh, G. Tran, K. Mueller, K. Doytcheva, et al., Ichthyosis molecular fingerprinting shows profound TH17 skewing and a unique barrier genomic signature, J. Allergy Clin. Immunol. 143 (2) (2019) 604–618.
[24] A.S. Paller, Profiling immune expression to consider repurposing therapeutics for the Ichthyoses, J. Invest. Dermatol. 139 (3) (2019) 535–540.
[25] A.S. Paller, Y. Renert-Yuval, M. Suprun, H. Esaki, M. Oliva, T.N. Huynh, et al., An IL-17-dominant immune profile is shared across the major orphan forms of ichthyosis, J. Allergy Clin. Immunol. 139 (1) (2017) 152–165.